Amplifier-assisted Waveguide Sensing toward Breath-gas Analysis

LI, Wenying
Department of Applied Science for Electronics and Materials, Kyushu University

HAN, Yu
Department of Applied Science for Electronics and Materials, Kyushu University : Graduate Student

CHEN, Zanhui
Department of Applied Science for Electronics and Materials, Kyushu University : Graduate Student

WANG, Leiyun
Department of Applied Science for Electronics and Materials, Kyushu University : Graduate Student

他

https://doi.org/10.15017/4479144

出版情報：九州大学大学院総合理工学報告. 42 (1), pp.19-26, 2020-09. 九州大学大学院総合理工学府
バージョン：
権利関係：

九州大学大学院総合理工学府報告
第 42 巻 第 1 号 19-26 頁 令和 2 年 9 月

Engineering Sciences Reports, Kyushu University
Vol. 42, No. 1, pp. 19-26, SEP, 2020

Amplifier-assisted Waveguide Sensing toward Breath-gas Analysis

Wenying LI[*1,†] Yu HAN[*1] Zanhui CHEN[*1] Leiyun WANG[*1]
Haisong JIANG[*2] and Kiichi HAMAMOTO[*2]
[†]E-mail of corresponding author: ri.uenin.271@s.kyushu-u.ac.jp

(Received July 31, 2020, accepted August 7, 2020)

We have proposed compact breath sensing device by using optical waveguide. As there is an inevitable huge loss in the waveguide, we have proposed and demonstrated optical amplifier-assisted scheme so as to compensate the waveguide propagation loss. One important issue of the amplifier-assisted scheme is the amplifier noise at sensing light wavelength. The significant accumulated amplifier noise may surpass the sensing light intensity and prevent ppm-order gas sensing. In this work, we calculated the necessary light intensity of the injected light into the fiber by taking account of the influence of amplifier noise. In addition, we have verified the proposed condition in experiment. As a result, the actual 3% CO_2 was successfully detected.

Key words: *Breath sensing, Optical waveguide, Amplifier-assisted cavity ring-down spectroscopy*

1. Introduction

Population aging problem has become one of the significant social problem. Because of this problem, the demand of daily and easy health-check system for elder people is considered to be important [1]. Especially home-based health monitor is desired [2]. Breath sensing [3-5] is available for the daily and easy health check because exhaled breath contains a lot kinds of disease markers [6, 7]. People only need breathing-out toward the sensor. The density of each disease marker in breath is analyzed at the time.

For home-use, breath sensor is desired to realize hand-held size, several diseases detection at one time, and quick response within a few seconds. Up to now, several types of breath sensors [8-19] have been researched. Among them, sensor based on infrared absorption spectroscopy [20] has the possibility to sense several kinds of gases at the same time [21-23]. This is because each gas has its own eigen absorption peak in wavelength [24]. For sensing ppm-order gas component in breath by using infrared absorption, an extremely long optical sensing path of several km is needed for sufficient light absorption (typically 3 dB)[22]. To achieve the effectively long length sensing path (corresponding km order), CRDS (cavity ring-down spectroscopy) [25] has been proposed. In CRDS system, km length sensing path is realized by using internal reflection at the cavity-edges. In case when the mirror reflectivity is set to be high to have 1,000 times reflection with a meter-long cavity for instance, the effective length may exceed km order [26]. One issue of the CRDS system as home-use sensor is its large size.

We have proposed breath sensor utilizing optical waveguide as the optical path for infrared absorption based on CRDS. This is because waveguide is capable for integrating several meter optical paths in a compact area

*1 Department of Applied Science for Electronics and Materials, Graduate student
*2 Department of Applied Science for Electronics and Materials

(1 cm^2) [27-29]. With sensing light propagating in waveguide for more than 1,000 times, the corresponding sensing path length is available for ppm-order breath sensing. One problem is the waveguide propagation loss. Huge amount of loss decreases the sensing light intensity. As most of the sensing light intensity is reduced due to the propagation loss, ppm-order breath sensing becomes hard to be realized. As a solution, we have proposed amplifier-assisted CRDS [30] to compensate the propagation loss. For hand-held breath sensor, SOA (semiconductor optical amplifier) is a candidate due to its capability of integration. To verify the effectiveness of the amplifier-assisted CRDS, we use an EDFA (Erbium-doped fiber amplifier) instead of the SOA inside CRDS system in this work. When EDFA is at a high pumping condition, ASE (amplified spontaneous emission) loops inside CRDS system and be amplified in the EDFA. Then, it starts self-lasing at a wavelength different from sensing light. Once self-lasing happens, sensing light looses the gain from EDFA. This is because most of the gain is attributed to lasing wavelength. We have proposed polarization direction control scheme [31] to suspend self-lasing by weakening the coherency condition. The coherency is a fundamental requirement of making oscillation in cavity (namely, ring-cavity here) in general. The result showed that the self-lasing intensity was suspended, and the gain was improved to 24 dB from 14 dB at the sensing light wavelength.

Whereas the self-lasing issue has been improved, there is still an important issue in the amplifier-assisted CRDS system. The amplifier noise which exists at sensing light wavelength is hardly eliminated. In ppm-order gas sensing, the amplifier noise loops inside the system with sensing light for more than 1,000 times. The significant accumulated noise intensity may surpass the sensing light intensity and prevent ppm-order breath sensing. Hence, the accumulated noise intensity influences the sensing ability of amplifier-assisted CRDS system directly. In this work, to evaluate the lowest gas sensing concentration of amplifier-assisted waveguide CRDS, we calculated the accumulated amplifier noise intensity at ppm-order gas sensing condition. Then we estimated the necessary injection light intensity for ppm-order gas sensing under the influence of the amplifier noise. The estimated results showed several kinds of ppm-order gases (CO_2, CH_4, NH_3, and CH_3COCH_3) are sensing-available by using the injection light intensity within 10 mW. Meanwhile, the actual 3% CO_2 sensing was also demonstrated experimentally to confirm the effectiveness of this proposal shown in this paper.

2. CRDS system for gas sensing

2.1 Principle of CRDS

In general, a volatile gas (target gas) has its own eigen absorption wavelength at infrared band [32]. Table 1 summarized the breath content in exhaled breath, their absorption wavelength λ [μm], absorption cross-section σ [cm^2], concentration N [ppm], and the related disease [33-37].

Table 1 Disease markers in human breath

Breath content	λ [μm]	N [ppm]	σ [cm^2]	Related disease
CH_4	1.65	2-10	1.6×10^{-20}	Intestine disease
NH_3	1.51	0.5-5	2.5×10^{-20}	Liver disease
CH_3CO CH_3	1.68	1.7-3.7	3.6×10^{-22}	Diabetes
CO	1.57	3.3-5.4	2.2×10^{-23}	Diabetes

To detect the target gas concentration in exhaled breath, km-order length of sensing path is needed [22]. One attractive technique to reduce this km-order length down to below 1 m is known as CRDS method. Figure 1 shows the schematic configuration of the general CRDS system. The gas-cell has high reflection mirrors at the both ends of the gas-cell. The high reflection mirrors are used to reflect the sensing light inside the gas-cell. When the reflection happens for more than 1,000 times in a 1 m length gas-cell for instance, the corresponding sensing path length reaches to the effective length of km-order. During each reflection, slight portion of the not-reflected (therefore transmitted) light leaks out from the gas-cell through the high reflection mirror [38]. The measurement is carried to detect this leak-out light intensity. The example measurement result (light intensity as a function of time) is shown in the right-hand side of Fig. 1. The light intensity decreases because of the leak-out

light from the mirror at the gas-cell ends. This situation happens even for “no-gas in gas-cell” situation. In the condition of “gas in gas-cell”, the light intensity decreases faster than the case of “no-gas” due to the gas absorption. Here, the cavity ring-down time [39] τ and τ_{gas} are defined as follows: the time that light intensity decreases to the criteria level (normally 1/e) (black dash-line in Fig. 1). And τ and τ_{gas} are the cavity ring-down times for “non-gas in gas-cell” and “gas in gas-cell” situation, respectively. The target gas concentration N [ppm] is estimated by using the cavity ring-down times as [40, 41]:

$$N=\left(\frac{1}{\tau_{gas}}-\frac{1}{\tau}\right)\times\frac{RT}{oc\times P\times NA\times 10^{-9}} \quad (1)$$

c [cm/μs] is light speed. Equation (1) shows that gas concentration is detected by measuring the sensing time in CRDS system. Based on the analysis above, CRDS system is capable for ppm-order gas sensing.

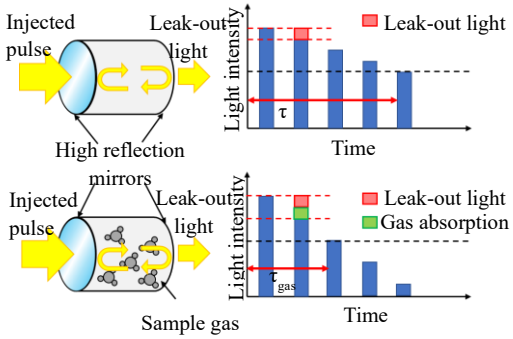

Fig. 1 Illustration of general CRDS (cavity-ring-down system).

The problem of general CRDS as hand-held sensor is its large gas-cell size. To realize hand-held sensor, we have proposed high-mesa waveguide [42] as the optical sensing path instead of gas-cell. This is because waveguide has a potential of integrating a long optical path in a compact area. When sensing light propagates in the high-mesa waveguide, a portion of light goes out of the waveguide. This portion of light intensity is used for gas absorption. Gas absorption happens by using waveguide as the sensing path. Hence, waveguide with high-reflection films on both facets is suitable in CRDS instead of general gas-cell for hand-held sensor.

2.2 Amplifier-assisted waveguide CRDS

In waveguide CRDS, waveguide has high-reflection films on both facets. Sensing light is reflected rapidly inside the waveguide. One problem is that, waveguide has propagation loss. Most of the injected sensing light is reduced due to the propagation loss. For instance, a 1 m length waveguide has 2 dB propagation loss. When light reflecting inside the waveguide exceeds 1,000 times for ppm-order gas sensing, the accumulated loss may reach to 2,000 dB. Breath sensing is impossible with this huge loss. To solve this problem, we have proposed amplifier-assisted CRDS. In amplifier-assisted CRDS, waveguide has no high-reflection film. The sensing light at the outbound of the waveguide is guided to an optical amplifier to compensate the waveguide propagation loss. After amplification, the sensing light is leaded to the inbound of the waveguide. This waveguide configuration; however; enclose the sensing light into a loop without leak-out light. It is impossible; therefore; to monitor the leak-out light intensity decrease as CRDS. As a solution, optical couplers are used to connect the output port of the amplifier and the inbound of the waveguide. The experimental set-up of amplifier-assisted CRDS is shown in Fig. 2 (a). In this experimental set-up, an EDFA (Erbium-doped fiber amplifier) is set inside the CRDS to demonstrate the effectiveness of the amplifier-assisted CRDS. Two optical couplers are used to guide the sensing light. The injected sensing light-pulse is guided to the inbound of the waveguide via coupler 1. The light coming out from the outbound of the waveguide is amplified by EDFA. Then, most of the sensing light is leaded back to the inbound of the waveguide via coupler 2 and 1. A portion of “leak-out light” is monitored via one output branch of the coupler 2. The amount of leak-out light is controlled by the branch ratio of coupler 2.

In this experiment, sensing light is at 1572 nm wavelength. This wavelength is the absorption wavelength of CO_2, which is a major content in human breath. Figure 2 (b) are the amplifier-assisted CRDS results (light intensity as a function of time when the injected light intensity was 1 mW). The orange pulse-trains correspond to the result of “before amplification” situation. The blue pulse-trains

correspond to the result of "after amplification" situation. Without amplification, light intensity decreased immediately. It only looped in waveguide for 3 times. When EDFA provided 5 dB gain and compensated part of the propagation loss, the looping time increased to 16 from only a few. These results lead to the sensing path length extending more than 5 times than that without amplification.

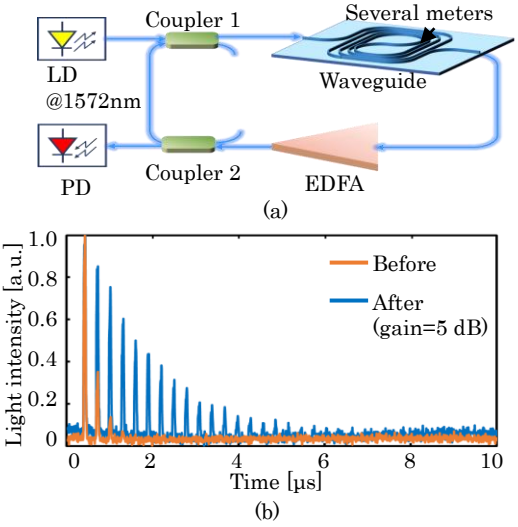

Fig. 2 The experimental set-up of amplifier-assisted CRDS and its results. (a) Experimental set-up, and (b) experiment results before and after amplification.

3. Issues in amplifier-assisted CRDS

Amplifier is used in waveguide CRDS to compensate the waveguide propagation loss. As amplifier gain increasing, the sensing light loops in waveguide for more times. The corresponding sensing path length increases. Amplifier inside CRDS; however; cause the self-lasing issue and the amplifier noise issue. In this session, we will discuss about these two issues and their solutions.

3.1 Self-lasing issue and solution

Amplifier is used inside a closed loop as shown in Fig. 2 (a). This configuration; however; may result in self-lasing when EDFA is at high pumping condition [43]. Figure 3 shows the optical spectrum of the amplifier-assisted CRDS under different pumping current of EDFA. Sensing light wavelength was at 1572 nm. As shown in the figure, self-lasing happened at 1564 nm wavelength. It seems that the self-lasing happened when injection current of the pumping LD in the EDFA was increased from 100 mA. As is indicated, the light intensity at self-lasing wavelength increased from -53 dBm to -7 dBm whereas the intensity at sensing light wavelength kept at -24 dBm.

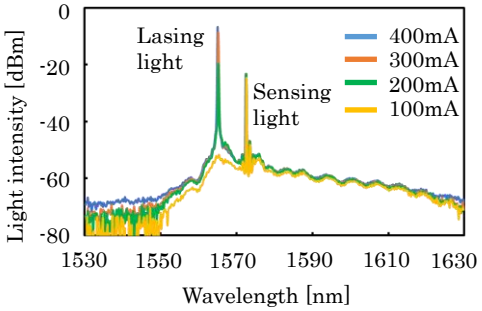

Fig. 3 Optical spectrum of amplifier-assisted CRDS at different EDFA pumping condition.

Once this self-lasing happens, sensing light is not amplified sufficiently because most of the amplifier gain is attributed to the lasing wavelength. The gains that EDFA provided to the sensing light and to the self-lasing light are shown in Fig. 4. Blue line is the gain that EDFA provides in single path optical system. Orange and green lines are the gains of the sensing light and the self-lasing light, respectively. As EDFA pumping current increasing, gain at the self-lasing wavelength increased from 15 dB to 22 dB, while the gain at the sensing light wavelength kept at 14 dB.

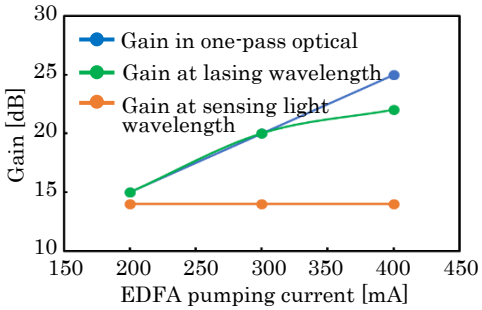

Fig. 4 EDFA gain at self-lasing wavelength, signal wavelength, and in single pass optical system.

The "first seed" of the self-lasing is the ASE (amplified spontaneous emission). When the Er^{3+} is pumped to produce a population inversion in EDFA, ASE is generated due to the spontaneous emission. ASE travels inside the amplifier-assisted CRDS. If the travelling ASE share the same frequency, phase, and polarization direction, the "coherency" condition is secured. Under the coherency condition, self-lasing happens when the

travelling ASE intensity reaches lasing threshold. To suspend the self-lasing, we propose polarization direction control scheme. This method is with changing the polarization direction of the travelling light wave to weaken the coherency condition. Figure 5 shows the experimental system of the polarization direction control scheme. A 3-stage polarization rotator with a polarizer, a 1/4 wave plate and a 1/2 wave plate is set into the cycle loop after EDFA. The ASE coming out from EDFA is non-linear polarization light. The polarizer is used to alter the ASE polarization state to linear polarization. The direction of the linear polarization light is changed by rotating the 1/2 wave plate. The 90° rotation of the polarization direction mostly weaken the coherency condition. Hence, self-lasing is suspended.

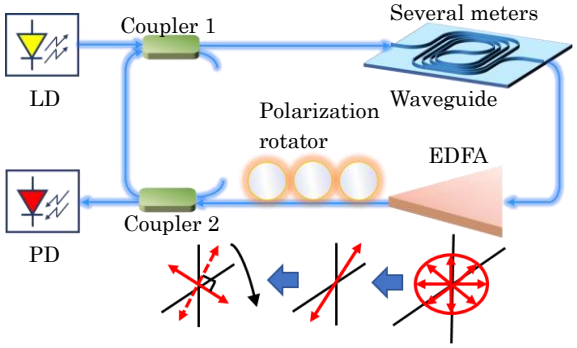

Fig. 5 Experimental system of polarization direction control scheme.

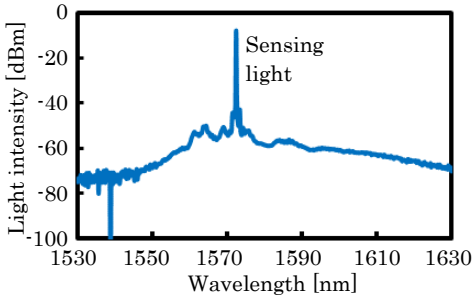

Fig. 6 Optical spectrum of polarization direction control scheme.

The result of the polarization direction control scheme is confirmed by using optical spectrum from the output port of coupler 2. The result is shown in Fig. 6. The self-lasing intensity was suspended below -50 dBm. We estimated that the gain at sensing light wavelength increased to 24 dB from 14 dB.

3.2 Amplifier noise issue and solution

Whereas self-lasing issue was solved, the amplifier noise is a serious problem in the amplifier-assisted CRDS. The amplifier noise mainly comes from four parts [44]: (a) Shot noise caused by amplified signal light; (b) Shot noise caused by spontaneous emission light; (c) Beat noise between signal light and spontaneous emission light; and (d) Beat noise between spontaneous emission light. Among these four kinds of amplifier noises, noise (a) and (c) exist in the same wavelength with the sensing light. These two kinds of noises are hardly eliminated. The noise intensity is accumulating while these noise looping inside the CRDS. In ppm-order gas sensing, after more than 1,000 times looping, the accumulated amplifier noise intensity may exceed the sensing light intensity. The intensity of the accumulated amplifier noise; therefore; directly influences the sensing ability of the amplifier-assisted CRDS.

To evaluate the sensing ability of the amplifier-assisted CRDS, firstly, we calculate the intensity of the amplifier noise. It is calculated by the amplifier noise figure (*NF*) [45].

$$NF = \left(\frac{Signal}{Noise}\right)_{IN} / \left(\frac{Signal}{Noise}\right)_{OUT} \quad (2)$$

When we change the *NF* into log-scale in [dB], eq. (3) becomes as follows:

$$NF = [(Signal)_{IN} - (Signal)_{OUT}] - [(Noise)_{IN} - (Noise)_{OUT}] \quad (3)$$

The gain *G* [dB] is expressed by $(Signal)_{OUT}$ and $(Signal)_{IN}$ as:

$$G = (Signal)_{OUT} - (Signal)_{IN} \quad (4)$$

$(Noise)_{IN}$ [dBm] is the input thermal noise, which is expressed as:

$$(Noise)_{IN} = 10 \times \log_{10}(kTB \times 10^3) \quad (5)$$

Here, *k* is Boltzmann constant, *T* [K] is temperature, and *B* [Hz] is the bandwidth. Then the amplifier noise intensity $(Noise)_{OUT}$ is written as:

$$(Noise)_{OUT} = NF + G + 10 \times \log_{10}(kTB \times 10^3) \quad (6)$$

In this case, we take *NF* as 3 dB in the calculation, because in EDFA the quantum limit of *NF* is 3 dB when the population inversion occurs sufficiently [46]. Based on the co-doped materials of Erbium-doped fiber [45],

EDFA has a stable gain that ranges from 15 dB to 40 dB. So, we assume that the gain is stable at 20 dB in this calculation. At the condition of T = 298 K (25 ℃) and sensing wavelength λ = 1572 nm, $(Noise)_{OUT}$ is calculated as -43 dBm (i.e., 50 nW). Then the accumulated noise intensity I_n [dBm]is calculated as:

$$I_n = 10\times\log_{10}(n\times 50\times 10^{-6}) \quad (7)$$

where n is the times that the noise looping inside the system.

To realize ppm-order breath sensing by using amplifier-assisted CRDS, after n times looping, the sensing light intensity I_s [dBm] is required to be larger than the accumulated noise intensity I_n. I_s is calculated as:

$$I_s = 10\times\log_{10}\{I_0\times[\exp(\sigma NL\times\Gamma_{out})]^n\} \quad (8)$$

I_0 [mW]is the injection light intensity. l [cm] is the waveguide length and Γ_{out} [%] is the portion of light profiles that comes out of the waveguide for gas absorption [41]. The term of "exp ($\sigma NL\times\Gamma_{out}$)" donates to the gas absorption attenuation in one loop. The value of I_s is available to be enhanced by increasing the injection light intensity I_0. We used CO_2 as an example to calculate the necessary injection light intensity for different CO_2 concentration. The calculated results are shown in Fig. 7. In this calculation, the system loss and the amplifier gain were all set as 20 dB (ideal condition). The light intensity criteria was 0.9 [a.u.]. The criteria is in inverse proportion to the cavity ring-down number. A higher criteria (~1 [a.u.]) leads to less cavity ring-down number. By using the criteria as 0.9 in this estimation, the accumulated amplifier noise intensity is low. The blue line is the accumulated amplifier noise. The blue dot line is the "noise intensity+ 3dB". It is the light intensity level to distinguish the sensing light and the noise.

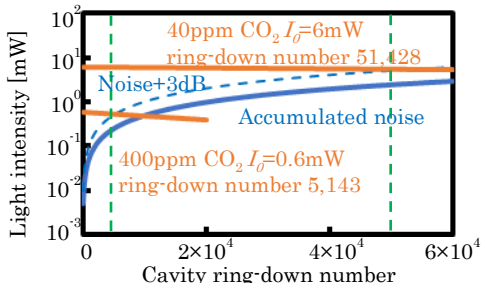

Fig. 7 The calculated results of the necessary injection light intensity for different CO_2 concentration.

When the injection light intensity increased from 0.6 mW to 6 mW, the detectable CO_2 concentration changed from 400 ppm to 40 ppm. The necessary injection light intensity I_0 for breath contents (CO_2, CH_4, NH_3, and CH_3COCH_3) are shown in Fig. 8.

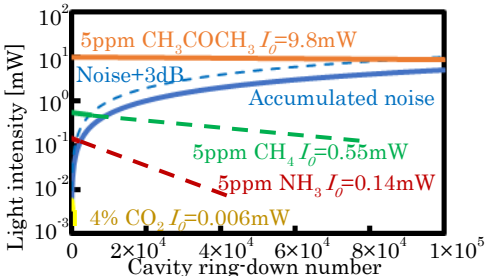

Fig. 8 The calculated results of the necessary injection light intensity for breath contents (CO_2, CH_4, NH_3, and CH_3COCH_3).

In this figure, the orange, green, red, and yellow line show the sensing light intensity decreasing tendency for CH_3COCH_3, CH_4, NH_3, and CO_2, respectively. Based on the estimation above, the concentration of CO_2 in human breath (40,000 ppm) is detectable with 0.006 mW injection light intensity. The CH_3COCH_3, CH_4, NH_3 in exhaled breath are detectable with injection light below 10 mW.

Most of the EDFA provides a stable gain when input light intensity is in between -40 dBm~-20 dBm [44,45,47]. The injection light intensity I_0 has an intensity limitation to ensure the stable gain of amplifier. The light intensity range of I_0 is estimated as: 0 dBm (1 mW) ≤ I_0 ≤ 10 dBm (10 mW), considering the loss of the waveguide (the loss is estimated as -20 dB). According to the analysis above, ppm-order gas concentration is detectable with the influence of amplifier noise. Amplifier-assisted CRDS is available for ppm-order gas sensing, as long as we control the injection light intensity.

4. CO_2 gas concentration measurement

Based on the calculation results above, one requirement is to use sufficient light intensity. For instance, I_0 is required to be more than 0.006 mW for CO_2. In this case, CO_2 concentration in human breath (40,000 ppm) is available for sensing. To confirm the actual availability, we tried 3% CO_2 gas sensing by using the amplifier-assisted CRDS with 1 mW

injection light-pulse. The light-pulse has a width of 10 ns and a period of 20 μs.

The sensing waveguide was silica high-mesa waveguide integrated on a Si wafer. Figure 9 (a) is structure of the integrated waveguide chip. The chip size is 0.9 cm × 0.9 cm. Figure 9 (b) is the structure of silica high-mesa waveguide. The length and width of the waveguide that was used in sensing experiment was 36.8 cm and 2.23 μm, respectively. The evaluated waveguide propagation loss was 0.02 dB/cm. Figure 9 (c) shows the waveguide simulated optical field. The light intensity out of waveguide (I_{out}) is estimated as 3% of the total light intensity.

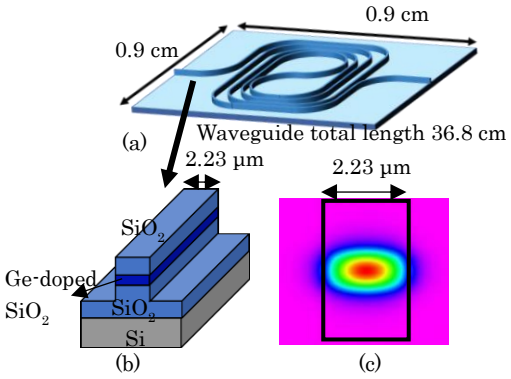

Fig. 9 High-mesa waveguide structure. (a) High-mesa waveguide chip, (b) waveguide structure, and (c) waveguide simulated optical field.

In order to analyze the light intensity of the pulse-train, we took the light intensity data of each pulse peak. By using these data, we draw the approximate line. The analyzed results are shown in Fig. 10. The blue dots and green triangles in Fig. 10 are the light intensity data of "no CO_2" and "3% CO_2" situation, respectively. The orange line and the yellow line are the approximate lines. The cavity ring-down times for gas concentration measurement is defined by the light intensity criteria that we set. Here, the criteria level is set at the light intensity ~1/e (red line in Fig. 10). This is because this value is near to the normal criteria level 1/e and easy for cavity ring-down time measurement. The cavity ring-down times were estimated as 80.7 μs and 41 μs for "no CO_2" and "3% CO_2" situation, respectively. Because human breath contains 4% CO_2, in this work, the result of 3% CO_2 sensing indicates that the proposed amplifier-assisted CRDS enable breath sensing.

The estimated CO_2 concentration corresponds to be 1%, and the value was not exactly same with the injected gas condition. This difference may be because of the error in the accuracy of CO_2 density. The 3% CO_2 that injected into the gas chamber was not proper 3% so that the sensing error happened. We are now on the way of the analysis of this difference.

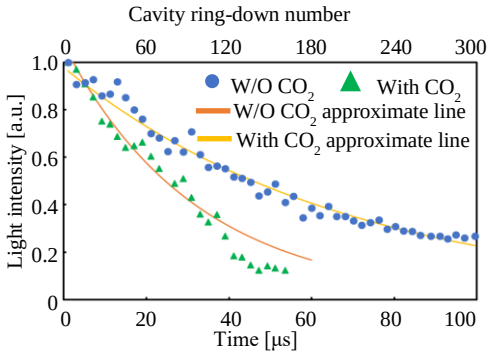

Fig. 10 3% CO_2 analyzed sensing results.

5. Conclusions

Amplifier-assisted waveguide scheme utilizing CRDS for gas sensing realizes ppm-order gas sensing. Amplifier inside CRDS; however; causes self-lasing issue and amplifier noise issue. These two issues prevent ppm-order gas sensing. We have proposed polarization direction control to suspend self-lasing. The results showed that self-lasing was suspended below -50 dBm. The intensity of accumulated amplifier noise directly influences the sensing ability of the amplifier-assisted waveguide scheme. The amplifier noise is hardly eliminated because it exists at sensing light wavelength. One requirement of gas sensing under the influence of amplifier noise is to use sufficient light intensity. Based on the calculation, injection light intensity within 10 mW is available for several kind of gas sensing (CO_2, CH_4, NH_3, and CH_3COCH_3). We successfully detected 3% CO_2 using 1 mW input sensing light intensity as a ring-down time difference (80.7 μs and 41 μs) based on the proposed amplifier-assisted CRDS. This result indicates that the amplifier-assisted CRDS is available for breath sensing.

6. Acknowledgments

This work has been supported in finance by SECOM Science and Technology Foundation. The authors greatly appreciate Drs. Mikitaka Itoh and Yasuaki Hashizume of NTT for their technical discussion and support.

References

1) S. Ogura, and M.M. Jakovljevic, Front. in public health, **6**, 335 (2018).
2) C.A. Mair, A.R. Quinones, and M.A. Pasha, The Gerontol., **56**(4), 687-701 (2016).
3) T.H. Risby and S.F. Solga, Appl. Phys. B, **85**(2-3), 421-426 (2006).
4) M. Murtz, Opt. & phontonics news, **16**(1), 30-35 (2005).
5) G. V. Basum, H. Dahnke, D. Halmer, P. Hering, and M. Murtz, Appl. Phys., **95**(6), 2583-2590 (2003).
6) N. Marczin, *Disease Markers in Exhaled Breath*, M. Yacoub, ed., Marcel Dekker, New York (2003) Chap. 1.
7) C. Wang, and P. Sahay, Sens., **9**(10), 8230-8262 (2009).
8) H. Gatty, G Stemme, and N. Roxhed, Micromach., **9**(12), 612 (2018).
9) W. Shin, T. Itoh, and N. Izu, Synth., **8**(4), 214-222 (2015).
10) H. Wakana, M. Yamada, and M. Sakairi, 2018 IEEE Sens., 1-4 (2018).
11) D. Wang, Q. Zhang, Md. Hossain, and M. Johnson, IEEE Sens. J., **18**(11), 4399-4404 (2018).
12) P. Sanchez, C. Zamarreno, M Hernaez, I. Matias, and F. Arregui, 2014 IEEE Sens., 1142-1145 (2014).
13) Z.H. Chen, W.Y. Li, Y. Han, H.S. Jiang, and K. Hamamoto, Jpn. J. of App. Phys., **58**(SJ), SJJD03 (2019).
14) R. Takasu, Fujitsu, **61**(1), 47-51 (2010). [in Japanese]
15) H. Miki, F. Matsubara, S. Nakashima, S. Ochi, K. Nakagawa, M. Matsuguchi, and Y. Sadaoka, Sens. and Actuators B: Chem., **231**, 458-468 (2016).
16) O. Tsuboi, S. Momose, and R. Takasu, Fujitsu Sci. Tech., **53**(2), 38-43 (2017).
17) F. Loizeau, H. Lang, T. Akiyama, S. Gautsch, P. Vettiger, A. Tonin, G. Yoshikawa, C. Gerber, and N. Rooij, Tech. Dig. IEEE MEMS, 621-624 (2013).
18) K. Reddy, Y. Guo, J. Liu, W. Lee, M.K.K. Oo, and X. Fan, Sens. and Actuators B: Chem., **159**(1), 60-65 (2011).
19) K. Bodenhofer, A. Hierlemann, G. Noetzel, U. Weimar, and W. Gopel, Anal. Chem., **68**(13), 2210-2218 (1996).
20) T. Iwata, T. Katagiri, and Y. Matsuura, Sens., **16**(12), 2058 (2016).
21) L. Tombez, E. Zhang, J. Orcutt, S. Kamlapurkar, and W. Green, Opt., **4**(11), 1322-1325 (2017).
22) K. Namjou, C. B. Roller, T. E. Reich, J. D. Jeffers, G. L. Mcmillen, P. J. Mccann, and M. A. Camp, App. Phys. B, **85**, 427-435 (2006).
23) H. Dahnke, D. Kleine, P. Hering, and M. Murtz, Appl. Phys. B, **72**(8), 971-975 (2001).
24) N. Gayraud, L.W. Kornaszewski, J.M. Stone, J.C. Knight, D.T. Reid, D.P. Hand, and W.N. MacPherson, App. Opt., **47**(9), 1269-1277 (2008).
25) M. Murtz, D. Halmer, M. Horstjann, S. Thelen, P. Hering, Spectrochim. Acta Part A, **63**, 963-969 (2005).
26) A. O' Keefe, and D.A. Deacon, Rev. of Sci. Instrum., **59**(12), 2544-2551 (1988).
27) W. Lai, S. Chakravarty, X. Wang, C. Lin, and R. Chen, Opt. lett., **36**(6), 984-986 (2011).
28) S. Kim et. al., IEEE Sens. J., **10**(1), 145-158 (2010).
29) A. Wilk, F. Seichter, S. Kim, E. Tutuncu, B. Mizaikoff, J.A. Vogt, U. Wachter, and P. Radermacher Anal. Bioanal. Chem., **402**(1), 397-404 (2012).
30) M. Tsujino, H. Hokazono, J. Chen, and K. Hamamoto, Tech. Dig. MOC, **H57**, 1-2 (2013).
31) W.Y. Li, Y. Han, Z.H. Chen, H.S. Jiang, and K. Hamamoto, Jpn. J. of App. Phys., **58**(SJ), SJJD01 (2019).
32) A. Barth, Biochim. et Biophys. Acta-Bioenerg., **1767**(9), 1073-1101 (2007).
33) D. Roccarina, EC. Lauritano, M. Gabrielli, F. Franceschi, V. Ojetti, and A. Gasbarrini, The Am. J. of gastroenterol., **105**(6), 1250-1256 (2010).
34) H. Zan, W. Tsai, Y. Lo, Y. Wu, and Y. Yang, IEEE Sens. J., **12**(3), 594-601 (2011).
35) K. Kao, M. Hsu, Y. Chang, S. Gwo, and J. Andrew Yeh, Sens., **12**(6), 7157-7168 (2012).
36) C. Turner, C. Walton, S. Hoashi, and M, Evans, J. of Breath Res., **3**(4), 046004 (2009).
37) P. Paredi, W. Biernacki, G. Invernizzi, S.A. Kharitnov, and P.J. Barnes, Chest, **116**(4), 1007-1011 (1999).
38) P. Zalicki, and R.N. Zare, J. Chem. Phys., **102**(7), 2708-2717 (1995).
39) H. Hokazono W.Y. Li, S. Enami, H.S. Jiang, and K. Hamamoto, IEICE Electron. Express, **12** (15),20150574 (2015).
40) D.F. Swinehart, J. of Chem. Educ., **39**(7), 333-335 (1962).
41) A. Laugier, and J. Garai, J. of Chem. Educ., **84**(11), 1832-1833, (2007).
42) J. Chen, H. Hokazono, D. Nakashima, M. Tsujino, Y. Hashizume, M. Itoh, and K. Hamamoto, Jpn. J. of App. Phys., **53**(2), 022502 (2014).
43) J. Chow, G. Town, B. Eggleton, M. Ibsen, K. Sugden, and I. Bennion, IEEE Photonics Tech. Lett., **8**(1), 60-62 (1996).
44) Ter-Mikirtychev, and Vartan, *Fundamentals of fiber lasers and fiber amplifiers*, Springer, Swizerland (2014) Chap. 7.
45) M. Nakazawa, *Erbium doped fiber amplifier*, Optronics, Tokyo (1999) Chap. 1 [in Japanese].
46) P.S. Dhami, and H.N. Shrivastava, *A textbook of biology*, Pradeep publications, Jalandhar (2015) pp. V/101.
47) E. Desurvire, D. Bayart, B. Desthieux, and S. Bigo. *Erbium-doped fiber amplifiers: device and system developments*, Wiley- Interscience, New York (2002) Chap. 5.